AD-A114 814 NAVAL RESEARCH LAB WASHINGTON DC F/G 20/3
INFLUENCE OF MAGNETIC SHEAR ON THE LOWER-HYBRID-DRIFT INSTABILI--ETC(U)
MAY 82 J D HUBA, G GANGULI
UNCLASSIFIED NRL-MR-4827 NL

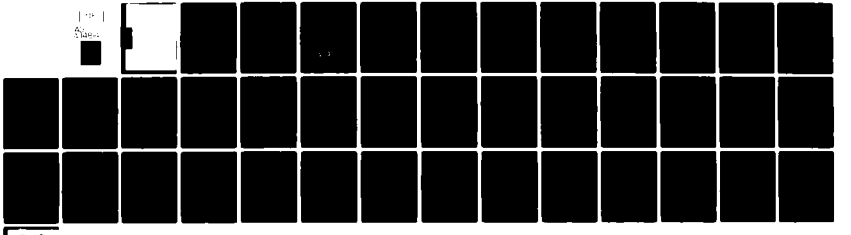

END
DATE FILMED
6 82
DTIC

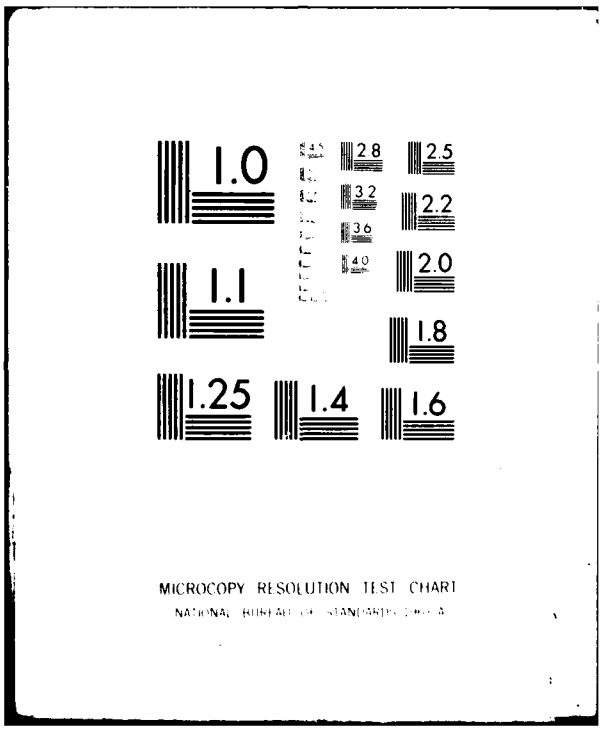
1.0
1.1
1.25
2.8
3.2
3.6
4.0
2.5
2.2
2.0
1.8
1.4
1.6
MICROCOPY RESOLUTION TEST CHART

SECURITY CLASSIFICATION OF THIS PAGE (When Data Entered)

REPORT DOCUMENTATION PAGE

READ INSTRUCTIONS BEFORE COMPLETING FORM

1. REPORT NUMBER: NRL Memorandum Report 4827	2. GOVT ACCESSION NO.: AD-A114814
3. RECIPIENT'S CATALOG NUMBER	
4. TITLE (and Subtitle): INFLUENCE OF MAGNETIC SHEAR ON THE LOWER-HYBRID-DRIFT INSTABILITY IN FINITE β PLASMAS	5. TYPE OF REPORT & PERIOD COVERED: Interim report on a continuing NRL problem.
	6. PERFORMING ORG. REPORT NUMBER
7. AUTHOR(s): J. D. Huba and G. Ganguli*	8. CONTRACT OR GRANT NUMBER(s)
9. PERFORMING ORGANIZATION NAME AND ADDRESS: Naval Research Laboratory, Washington, D.C. 20375	10. PROGRAM ELEMENT, PROJECT, TASK AREA & WORK UNIT NUMBERS: 61153N; RR0330244; 47-0884-0-2; NASA: W14365; 47-1447-0-2
11. CONTROLLING OFFICE NAME AND ADDRESS: Office of Naval Research, Washington, DC 22217; National Aeronautics and Space Admin., Washington, DC 20546	12. REPORT DATE: May 18, 1982
	13. NUMBER OF PAGES: 39
14. MONITORING AGENCY NAME & ADDRESS (if different from Controlling Office)	15. SECURITY CLASS. (of this report): UNCLASSIFIED
	15a. DECLASSIFICATION/DOWNGRADING SCHEDULE

16. DISTRIBUTION STATEMENT (of this Report)

Approved for public release; distribution unlimited.

17. DISTRIBUTION STATEMENT (of the abstract entered in Block 20, if different from Report)

18. SUPPLEMENTARY NOTES

*Present address: Berkeley Scholars, Inc., Springfield, VA 22150

This research was supported by ONR and NASA.

19. KEY WORDS (Continue on reverse side if necessary and identify by block number)

Drift instability
Reversed field plasma
Magnetic shear
Inhomogeneous plasmas

20. ABSTRACT (Continue on reverse side if necessary and identify by block number)

A self-consistent theory of the lower-hybrid-drift instability in finite β plasmas containing magnetic shear is presented. The important finite β effects included are (1) the coupling of electrostatic and electromagnetic oscillations and (2) the orbit modification of the electrons due to ∇B. It is found that the effect of electromagnetic coupling is a destabilizing influence on the instability in a sheared field. On the other hand, the effect of electron orbit modification (i.e.,

(Continues)

DD FORM 1 JAN 73 1473 EDITION OF 1 NOV 65 IS OBSOLETE
S/N 0102-014-6601

SECURITY CLASSIFICATION OF THIS PAGE (When Data Entered)

20. ABSTRACT (Continued)

electron ∇B drift-wave resonance) is a stabilizing influence. The key parameter which dictates which effect is more important is T_e/T_i. In the limit $T_e \ll T_i$, the electromagnetic effect dominates, while for $T_e \geq T_i$, the ∇B electron drift-wave resonance is more important. The relevance of these results to reversed field plasmas is discussed.

CONTENTS

INFLUENCE OF MAGNETIC SHEAR ON THE LOWER-HYBRID-DRIFT INSTABILITY IN FINITE β PLASMAS

I. INTRODUCTION

The lower-hybrid-drift instability is believed to be an important microinstability, in both space and laboratory plasmas, because of the anomalous transport properties associated with it.[1] This instability is driven by the diamagnetic current in an inhomogeneous plasma and is attractive because (1) it can be excited by modest density gradient (i.e., $L_n < (m_i/m_e)^{1/4} r_{Li}$ where L_n is the scale length of the density gradient and r_{Li} is the mean ion Larmor radius) and (2) it is relatively insensitive to the temperature ratio T_e/T_i (unlike, say, the ion acoustic instability).[2] The mode originally gained interest as a means to provide anomalous diffusion of particles in θ pinch experiments during late-time sheath broadening.[1,3,4] Subsequently, it has been applied to other laboratory devices, such as toroidal reversed field pinches[5,6] and compact torii,[7] and to magnetospheric plasmas.[8] Experimentally, the lower-hybrid-drift instability has been directly observed in a laboratory plasma[9] and has been suggested a mechanism to explain satellite observations of fluctuating electric fields in the earth's magnetopause[10] and magnetotail.[11]

At present, there is considerable interest in the lower-hybrid-drift instability in regard to its influence on the dynamics of reversed field plasmas. It is being applied to the field reversed experiments at Los Alamos[4,12] and to reconnection processes in the earth's magnetosphere.[8,13] One of the important features of a field reversed plasma (specifically, one containing a field null) is that β varies over an enormous range in the reversal region. To accurately describe lower-hybrid-drift waves in such a plasma, the analysis must include finite β effects.[2] The two important finite β effects that enter the

Manuscript submitted April 2, 1982.

problem are (1) the coupling of electrostatic and electromagnetic oscillations and (2) the orbit modification of the electrons due to ∇B. Aside from finite β, another potentially important feature in reversed field plasmas is magnetic shear; the reversing field could be sheared by a component of B which is parallel to the plasma current that generates the field reversal.

The initial study of the influence of magnetic shear on the lower-hybrid-drift instability considered electrostatic waves in a low β plasma using analytical analysis.[14] It was found that magnetic shear stabilized the instability for $L_s < L_n (r_{Li}/L_n + L_n/r_{Li})$ where L_s is the scale length associated with the magnetic shear. A numerical analysis of this problem was presented in Gladd et al. (1977).[5] Davidson et al. (1978)[6] extended previous analyses to finite β plasma. However, they considered the limit $T_e \to 0$ so that electron-wave resonances could be ignored. The important finite β effect retained was the coupling of electrostatic and electromagnetic oscillations. Recently, Huba et al. (1982)[15] have developed a theory of the instability in finite β and T_e plasmas containing magnetic shear. However, the results are restricted to the parameter regime $T_e \ll T_i$ and $\beta_e \ll 1$. Thus, to date, a general self-consistent theory of the lower-hybrid-drift instability in a finite β and T_e plasma containing a sheared magnetic field has not been developed. The purpose of this paper is to present such a theory.

The major results of this work are the following. The finite β effect arising from the coupling of electrostatic and electromagnetic perturbations can have a destabilizing influence on the instability in a sheared magnetic field. That is, as β is increased in certian parameter regimes, the growth rate of the instability increases. Physically, this

occurs because the fluctuating electric field associated with $\delta A_{\parallel}$ inhibits electron flow along the magnetic field which reduces the rate at which energy can be convected away from the localization region. The finite β effect of electron orbit modification has a stabilizing influence on the instability in a sheared field. This is due to a ∇B electron drift-wave resonance which is a dissipitative effect. The key parameter which dictates which finite β effect is more important is T_e/T_i. In the limit $T_e \ll T_i$ the electromagnetic coupling is dominant, while for $T_e > T_i$ the ∇B electron-wave resonance is more important.

The structure of the paper is as follows. In Section II we present the assumptions, equilibrium, and derivation of the equations which describe the lower-hybrid-drift instability in a finite β plasma containing magnetic shear. In Section III, the results are presented, both analytical and numerical. And finally, the last section summarizes the results and discusses the application of this work to reversed field plasmas. Details of the calculation are presented in Appendices A and B.

II. THEORY

A. Assumptions and Equilibrium

We consider a slab geometry plasma which contains inhomogeneties in the density and the magnetic field in the x-direction. The temperature is assumed constant for simplicity. Equilibrium force balance on an ion fluid element in the x-direction requires that $V_{iy} = V_{di}$ where $V_{di} = (v_i^2/2\Omega_i)\, \partial\, \ell n\, n/dx$ is the ion diamagnetic drift velocity, $v_i = (2T_i/m_i)^{1/2}$ is the ion thermal velocity and $\Omega_i = e\, B_o/m_i c$ is the ion Larmor frequency. The ion-diamagnetic velocity can be related to the mean ion Larmor radius and the scale length of the density gradient by $V_{di}/v_i = r_{Li}/2L_n$ where $r_{Li} = v_i/\Omega_i$ and $L_n = (\partial \ell n\, n/\partial x)^{-1}$ is the density gradient scale length. We consider magnetized electrons while the ions are kept unmagnetized. This is reasonable in treating the lower-hybrid-drift instability since we are considering waves such that $\Omega_i << \omega << \Omega_e$ and $k^2 r_{Li}^2 >> 1$. We assume that the plasma is weakly inhomogeneous, i.e, $r_{Le}^2\, (\partial \ell n\, n/\partial x)^2 << 1$ and $r_{Le}^2\, (\partial \ell n\, B/\partial x)^2 << 1$. The plasma β is arbitrary. The inhomogeneous ambient magnetic field is given by

$$\underline{B}(x) = B_o\{[1 + (x-x_o)/L_B]\hat{e}_z + (x-x_o)/L_s\, \hat{e}_y\} \qquad (1)$$

in the vicinity of x_o (i.e. $(x-x_o)/L_s << 1$ and $(x-x_o)/L_B << 1$ where $L_s = (\partial\Phi/\partial x)^{-1}$, $\Phi = \tan^{-1}(B_y/B_z)$ and $L_B = (\partial\, \ell n\, B_z/\partial x^{-1}))$. Thus, L_s is the scale length characterizing the magnetic shear and L_B characterizes the magnetic field gradient scale length.

In the absence of any field inhomogeneities, the field configuration is $\underline{B} = B_o\, \hat{e}_z$. The plasma described above is unstable to the kinetic lower-hybrid-drift instability when $1 > V_{di}/v_i > (m_e/m_i)^{1/4}$.[16] The instability

is driven by by cross-field current and is excited via an ion-wave resonance (i.e., invers Landau damping). The waves are characterized at maximum growth by $\omega_r \sim k_y V_{di} \lesssim \omega_{\ell h}$, $\gamma \lesssim \omega_r$, $k_y \rho_{es} \approx \sqrt{2}$, and $\underline{k} \cdot \underline{B} = 0$ where $\rho_{es} = (2T_i/m_e)^{1/2}/\Omega_e$. For modes such that $\underline{k} \cdot \underline{B} \neq 0$ (i.e., $k_\parallel \neq 0$) electron Landau damping reduces the growth rates or stabilizes them, depending on the magnitude of $k_\parallel$.

The above description of the plasma is significantly modified by introducing a shear in the magnetic field as given in Eq. 1. The magnetic field rotates in the y-z plane (see Fig. 1) as a function of x. At x_o we see that $k_\parallel = 0$ while at $x = x_1$, $k_\parallel \neq 0$. Thus the dispersive properties of the plasma are also a function of x. We introduce the effect of the magnetic shear (i) locally through $k_z \rightarrow k_z(x) = k_{zo} + k_y(x-x_o)/L_s$ and (ii) globally by replacing ik_x by $\partial/\partial x$. We note that the magnetic shear distorts the particle orbits in a uniform magnetic field and introduces a kinematic drift term.[17] The orbital effects of shear will be considered elsewhere.

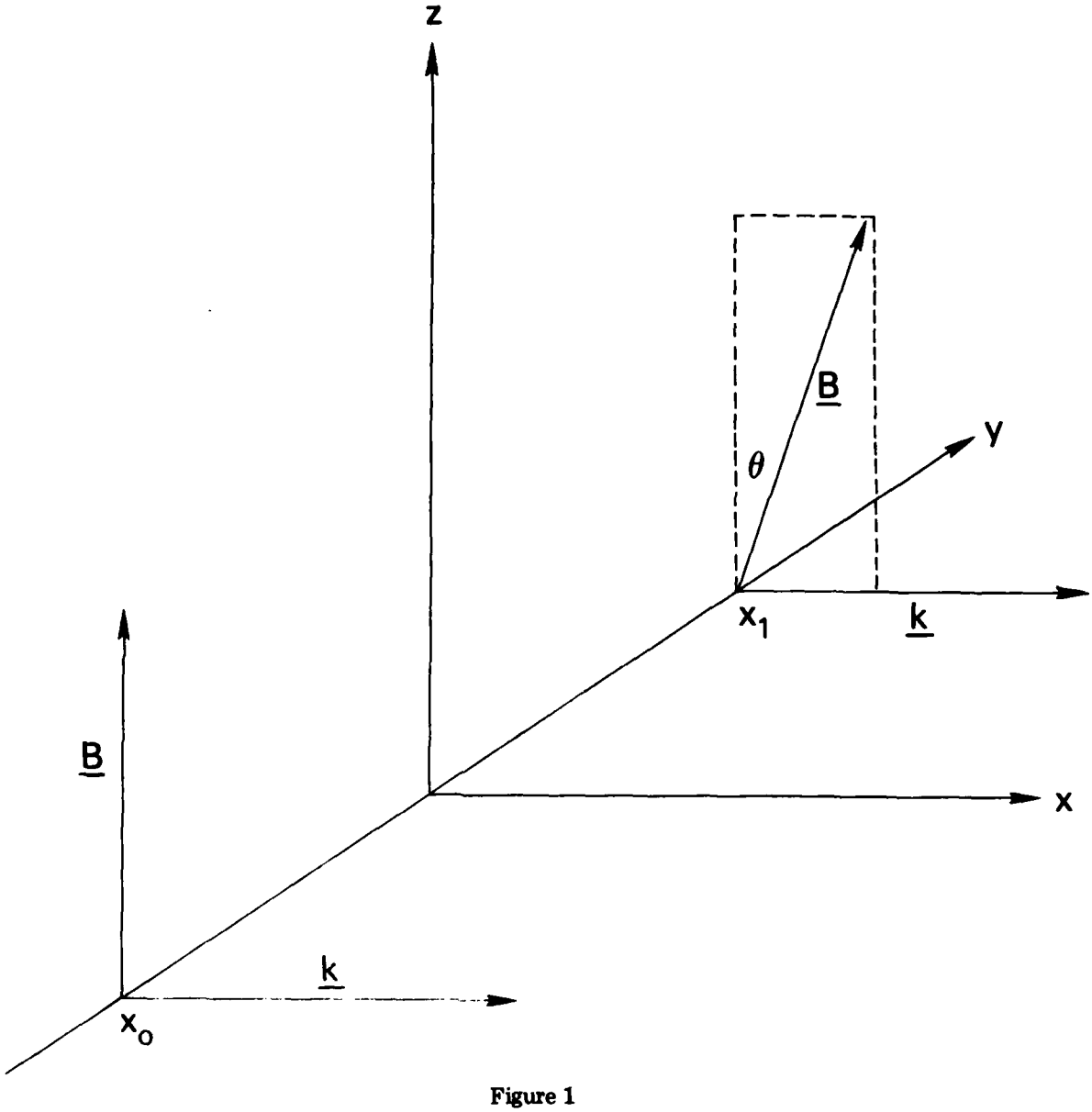

Figure 1

Schematic ot a sheared magnetic field.

B. Dispersion Equation

An outline of the derivation of the dispersion equation which describes the lower-hybrid-drift instability in a finite β plasma containing a sheared magnetic field is presented. Details of the analysis are presented in Appendices A and B. The Maxwell equations for the perturbed fields are

$$\nabla \cdot \delta\underset{\sim}{E} = 4\pi\, \delta\rho \tag{2}$$

$$\nabla \times \delta\underset{\sim}{B} = \frac{4\pi}{c}\, \delta\underset{\sim}{J} + \frac{1}{c}\frac{\partial \delta\underset{\sim}{E}}{\partial t} \tag{3}$$

where $\delta\rho$ and $\delta\underset{\sim}{J}$ are the perturbed charge density and current, respectively. Equations (2) and (3) can be rewritten as

$$\nabla^2\, \delta\phi = 4\pi \sum_{\alpha} e_{\alpha} \delta\, n_{\alpha} \tag{4}$$

$$\nabla \times \nabla \times \delta\underset{\sim}{A} + \frac{1}{c^2}\frac{\partial^2 \delta\underset{\sim}{A}}{\partial t^2} + \frac{1}{c}\nabla \frac{\partial \delta\phi}{\partial t} = \frac{4\pi}{c} \sum_{\alpha} \delta\underset{\sim}{J}_{\alpha} \tag{5}$$

where

$$\delta\underset{\sim}{B} = \nabla \times \delta\underset{\sim}{A} \tag{6}$$

$$\delta\underset{\sim}{E} = -\nabla\delta\phi - \frac{1}{c}\frac{\partial \delta\underset{\sim}{A}}{\partial t} \tag{7}$$

relate the perturbed fields to the perturbed potentials, and

$$\delta n_{\alpha} = \int d^3v\, \delta f_{\alpha} \tag{8}$$

$$\delta \underset{\sim}{J} = e_\sigma \int d^3v \; \underset{\sim}{v} \; \delta f_\sigma \tag{9}$$

where δf_σ is the perturbed distribution function of the σ species. We assume that perturbed quantities vary as exp [i ($\underset{\sim}{k} \cdot \underset{\sim}{x} - \omega t$)] where $\underset{\sim}{k} = k_x \hat{e}_x + k_y \hat{e}_y + k_z \hat{e}_z$ and $k_x = -i \, \partial/\partial x$ is an operator. Equations (4) and (5) becomes

$$k^2 \; \delta\phi = 4\pi e \; (\delta n_e - \delta n_i) \tag{10}$$

$$k^2 \; \delta \underset{\sim}{A} = - \frac{4\pi}{c} \; \delta \underset{\sim}{J}_e \tag{11}$$

In writing Eqs. (10) and (11) we have also used the Coulomb gauge ($\nabla \cdot \delta \underset{\sim}{A} = 0$) and have assumed $\omega^2 << c^2k^2$. Only the electrons contribute to perturbed current in Eq. (11) since $\omega_{pi}^2 << c^2k^2$.

We now calculate δn_σ and $\delta \underset{\sim}{J}_e$ as functions of the perturbed potentials using linear Vlasov theory. Details of this calculation are given in the Appendix A. Making use of δn_σ and $\delta \underset{\sim}{J}_e$, we write Eqs. (10) and (11) as

$$D_{\phi\phi} \; \delta\phi + \frac{k}{k_y} D_{\phi x} \; \delta A_x + D_{\phi z} \; \delta A_z = 0 \tag{12}$$

$$\frac{k_y}{k} D_{x\phi} \; \delta\phi + D_{xx} \; \delta A_x + \frac{k_y}{k} D_{xz} \; \delta A_z = 0 \tag{13}$$

$$D_{z\phi} \; \delta\phi + \frac{k}{k_y} D_{zx} \; \delta A_x + D_{zz} \; \delta A_z = 0 \tag{14}$$

In order to solve Eqs. (12) - (14) we assume that $k_x^2 << k_y^2$ and expand each D about this parameter. That is, we write $D = D^{(0)} + (k_x/k_y)\, D^{(1)} + (k_x^2/k_y^2)\, D^{(2)}$. Analysis of the relative magnitude of each term in D indicates that the first order term can be neglected when $\omega/k_y v_e << 1$. Since we are interested in modes which have $\omega \lesssim k_y v_i$, this criteria is satisfied when $T_e/T_i >> (m_e/m_i)^{1/2}$. In the opposite limit $T_e/T_i << (m_e/m_i)^{1/2}$, the first order terms cancel exactly. Thus, we can write $D = D^{(0)} + (k_x^2/k_y^2)D^{(2)}$. Making use of this relationship and eliminating δA_x and δA_z from Eq. (12), we arrive at the following second-order differential equation

$$p(\omega,k_y,x)\,\frac{\partial^2\delta\phi}{\partial x^2} - q(\omega,k_y,x)k_y^2\,\delta\phi = 0 \qquad (15)$$

where p and q are derived and defined in Appendix B (Eqs. (B32) and (B34)). In writing Eq. (15) we have made the indentification $k_x^2 \to \partial^2/\partial x^2$ and retained terms only to order k_x^2/k_y^2. Thus, the sixth-order set of differential equations in Eq. (12) - (14) is reduced to a second-order differential equation. The crucial assumption in this analysis is $k_x^2 << k_y^2$.

Although Eq. (15) is very complex, in general, its form is simple and amenable to numerical analysis. Moreover, in certain parameter regimes, analytical solutions are possible. We now turn our attention to solution of Eq. (15). We first present an analytical analysis which highlights the various influences of finite β on the lower-hybrid-drift instability in a sheared magnetic field. We then present numerical results for a broader parameter regime.

III. Results

A. Analytical Results

Earlier analytical studies of the influence of magnetic shear on the lower-hybrid-drift instability in a finite β plasma wave were restricted to the cold electron limit ($T_e \to 0$). Recently Huba et al. (1982)[15] extended previous analytical results to include ∇B electron drift-wave resonances. We present the major result of this analysis to shed light on the nature of the two important finite β effects: electromagnetic coupling and ∇B drift-wave resonances.

Huba et al. (1982) derive the following dispersion equation which describes the lower-hybrid-drift instability in a finite β plasma containing a sheared magnetic field for the lowest order mode

$$D(\omega,k) = 1 + k^2\hat{\rho}_{es}^2/2 - \frac{k_y V_{di}}{\omega} + i\{\sqrt{\pi}\left(\frac{\omega - k_y V_{di}}{k v_i}\right) + \frac{k v_i}{\omega_{pi}} - \frac{\omega_{pe}}{\omega}\frac{\rho_{es}}{L_s} + \pi \frac{T_i}{T_e} s_e \exp(-s_e)\Lambda_o^2\} \tag{16}$$

where

$$\Lambda_o = J_o(\zeta_r) - \frac{\sqrt{2\beta_i}}{k\rho_{es}}\left(\frac{T_e}{2T_i}\right)^{1/2} s_e^{1/2} J_1(\zeta_r)$$

and $\hat{\rho}_{es}^2 = \rho_{es}^2/(1 + \beta_i/2)$, $\rho_{es}^2 = 2T_i/m_e\Omega_e^2$, $V_{di} = (v_i^2/2\Omega_i)\,\partial\,\ell n\, n/\partial x$, $\omega_{p\sigma}^2 = 4\pi n e^2/m_\sigma$, $\zeta_r = k_y r_{Le} s_e^{1/2}$, and $s_e = (\omega_r/k_y V_{di})(2/\beta_e)$. This equation is derived based upon the following assumptions: $2\omega_{pi}^2/k^2v_i^2 \gg 1$, $\omega_{pe}^2 \gg \Omega_e^2$, $s_e \gg 1$ $\omega/k_\parallel v_e \gg 1$ $k_y^2 r_{Le}^2 \ll 1$, $V_{di} \ll v_i$, $T_e \ll T_i$ and $\beta_i \ll 1$. The first imaginary term in Eq. (16) is the destabilizing term due to inverse ion Landau damping. The second imaginary term is the

stabilizing effect of magnetic shear. It's origin in the analysis is a term $\propto (k_\parallel/\omega)^2$ in the magnetized electron response. Physically, magnetic shear leads to stabilization since it allows wave energy to propagate away from the excitation region (i.e. where $k_\parallel = 0$). The final term is a damping term due to the electron ∇B drift-wave resonance

The real frequency is given by

$$\omega_r = k_y V_{di}/(1 + k^2\hat{\rho}_{es}^2/2) \tag{17}$$

where shear corrections to ω_r have been neglected. The mode is stabilized when Im $D(\omega,k) = 0$ or

$$\left(\frac{L_n}{L_s}\right)_{cr} = -\frac{\sqrt{\pi}}{1+k^2\hat{\rho}_{es}^2/2}\left(1 + \frac{\beta_i}{2k^2\rho_{es}^2}\right)\left(\frac{V_{di}}{v_i}\frac{1}{2}\frac{k^2\rho_{es}^2}{1+k^2\hat{\rho}_{es}^2/2} + \right. \tag{18}$$

$$\left. \sqrt{\pi}\,\frac{T_i}{T_e}\, s_e \exp(-s_e)\Lambda_o^2\right).$$

where the subscript refers to the critical value of L_n/L_s. The maximum value of the RHS of eq. (18) occurs for $k^2\hat{\rho}_{es}^2 \simeq k^2\rho_{es}^2 \simeq 2$ so that all wavenumbers are stable when

$$\left(\frac{L_n}{L_s}\right)_{cr} = \frac{\sqrt{\pi}}{4}\left(1 + \frac{\beta_i}{4}\right)\left[\frac{V_{di}}{v_i} + 2\sqrt{\pi}\,\frac{T_i}{T_e}\, s_e \exp(-s_e)\Lambda_o^2\right] \tag{19}$$

and $s_e = 1/\beta_e$.

Two interesting points concerning Eqs. (18) and (19) are the following First, the finite β_i dependence in the first term of Eqs. (18) and (19) arise from the electromagnetic correction due to $\delta A_\parallel$ (i.e, the transverse magnetic field fluctuations) The influence of this correction

is to increase the amount of shear necessary to stabilize the mode. That is as β_i increases, the shear length L_s necessary for stabilization decreases so that the mode is harder to stabilize. Physically, this occurs because of the fluctuating electric field associated with $\delta A_\parallel$ inhibits free streaming electron flow along the magnetic field which reduces the rate at which energy can be convected away from the localization region. Secondly the final term is Eq. (19) represents the resonant ∇B correction which is a damping effect. This term tends to decrease the amount of shear necessary to stabilize the mode. Thus, the finite β corrections have different influences on the shear stabilization criterion. Lossely speaking, electromagnetic effects are destabilizing (i.e. a stronger shear is needed to stabilize the mode from the $\beta = 0$ situation) while the resonant ∇B effects are stabilizing (i.e., a weaker shear is needed to stabilize the mode from the $\beta = 0$ situation)

B. Numerical Results

We now present numerical solutions of Eq. (15) for a variety of parameter regimes. We solve Eq (15) by first re-writing it as

$$\frac{\partial^2 \delta\phi}{\partial x^2} - Q(\omega, k_y, x)\ \delta\phi = 0 \tag{20}$$

where $Q = q/p$ and use a finite difference scheme (i.e Numerov method)[18] to obtain eigenvalues and eigenfunctions. The boundary conditions used are

$$\delta\phi(x) = \frac{1}{Q^{1/4}(x)} \cdot \exp\left[\pm i \int^{x} dy\ Q^{1/2}(y)\right] \text{ for } |x| \to \infty \tag{21}$$

and $$\frac{d\delta\phi}{\partial x} = 0 \text{ for } x = 0.$$

The sign of the WKB solution in Eq. (21) is chosen such that a damped solution is obtained in the limit $|x| \to \infty$. The integrals contained in Q are performed numerically using a Chebychev quadrature method.

Figure 2 is a plot of $\gamma/\omega_{\ell h}$ vs $k\rho_{es}$ for $V_{di}/v_i = 1.0$ $T_e/T_i = 1.0$ $\omega_{pe}/\Omega_e = 10.0$ and $L_n/L_s = 0.1$. We consider two values of β $\beta = 0.0$ and $\beta = 0.2$ The $\beta = 0.0$ curve (dashed curve) is the electrostatic result and is presented as a reference to aid in understanding the influence of finite β effects. Three $\beta = 0.2$ curves are presented: (1) $\delta_{em} \neq 0$, $\delta_{\nabla B} = 0$; (2) $\delta_{em} = 0$, $\delta_{\nabla B} \neq 0$; and (3) $\delta_{em} \neq 0$, $\delta_{\nabla B} \neq 0$. These conditions have the following meaning. In calculating Q we have arbitrarily included two coefficients δ_{em} and $\delta_{\nabla B}$. The parameter δ_{em} modifies the electromagnetic coupling term $(\delta_{em}\omega_{pe}/ck)$ and the parameter $\delta_{\nabla B}$ modifies the electron ∇B drift velocity $(\delta_{\nabla B} V_{Be})$. By chosing δ_{em} and $\delta_{\nabla B}$ equal to 0 or 1, we can understand how these

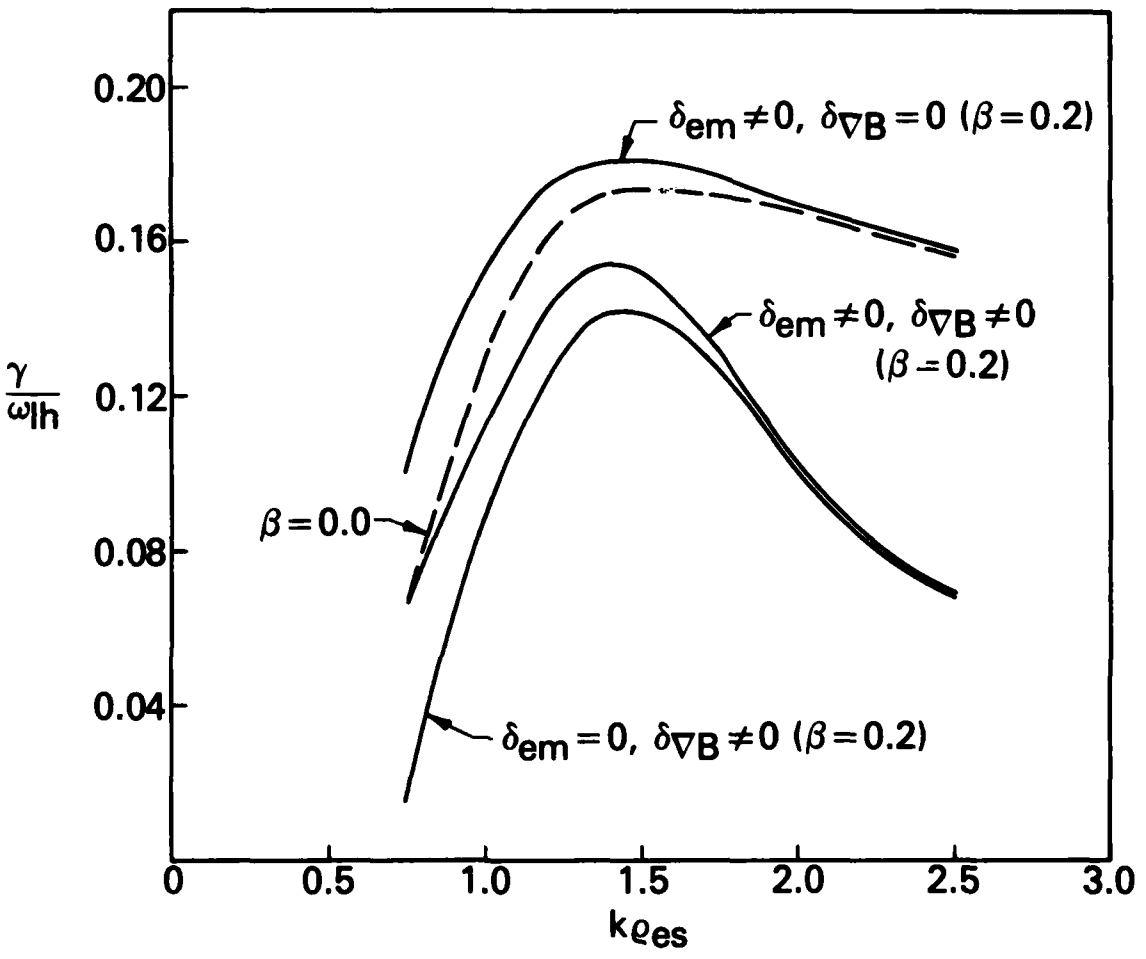

Figure 2

Plot of $\gamma/\omega_{\ell h}$ vs. $k\rho_{es}$ for $V_{di}/v_i = 1.0$, $T_e/T_i = 1.0$, $\omega_{pe}/\Omega_e = 10.0$ and $L_n/L_s = 0.1$. Two values of β are considered: $\beta = 0.0$ and $\beta = 0.2$. The parameters δ_{em} and $\delta_{\nabla B}$ refer to coefficients that modify the electromagnetic coupling term and the electron ∇B drift velocity (see text for detailed explanation).

finite β effects independently influence the instability in the presence of magnetic shear. That is, by setting $\delta_{em} = 1$ and $\delta_{\nabla B} = 0$, we retain electromagnetic coupling effects, but neglect electron ∇B orbit modification effects. Conversely, by setting $\delta_{em} = 0$ and $\delta_{\nabla B} = 1$, we retain electron ∇B orbit modification effects, but neglect electromagnetic coupling effects. Neither of these limits are self-consistent but are taken for pedagogical purposes. The self-consistent limit is $\delta_{em} = 1$ and $\delta_{\nabla B} = 1$. The top curve considers $\delta_{em} = 1$ and $\delta_{\nabla B} = 0$. Note that the influence of electromagnetic effects is to increase the growth rate relative to the $\beta = 0.0$ curve. This is most pronounced in the long wavelength regime ($k\rho_{es} < 1$) since ω_{pe}/ck is largest in this regime. The bottom curve considers $\delta_{em} = 0$ and $\delta_{\nabla B} = 1$. Note that the influence of the electron ∇B drift is to decrease the growth rate relative to the $\beta = 0.0$ curve. The enhanced damping, due to the dissipative electron ∇B drift-wave resonance, is strongest in the short wavelength regime ($k\rho_{es} > 1$). This is because the perpendicular resonant velocity ($v_{\perp r}$) is proportional to k^{-2} in this regime and, therefore, more electrons can participate in the resonance. Finally, the self-consistent result ($\delta_{em} = 1$ and $\delta_{\nabla B} = 1$) lies in between the two extreme limits. Electron ∇B damping dominates in the short wavelength regime while there is a balance of the electromagnetic and ∇B effects is the long wavelength regime. These results are consistent with those presented in Davidson et al. (1977).[2]

In Fig. 3 we plot $\gamma/\omega_{\ell h}$ vs. $k\rho_{es}$ for $V_{di}/v_i = 1.0$, $\omega_{pe}/\Omega_e = 10.0$, $L_n/L_s = 0.1$, $\beta = 0.2$ and two values of T_e/T_i: $T_e/T_i = 0.1$ and $T_e/T_i = 1.0$. The growth rates for these two curves are comparable; the only significant difference occurs in the short wavelength regime where the

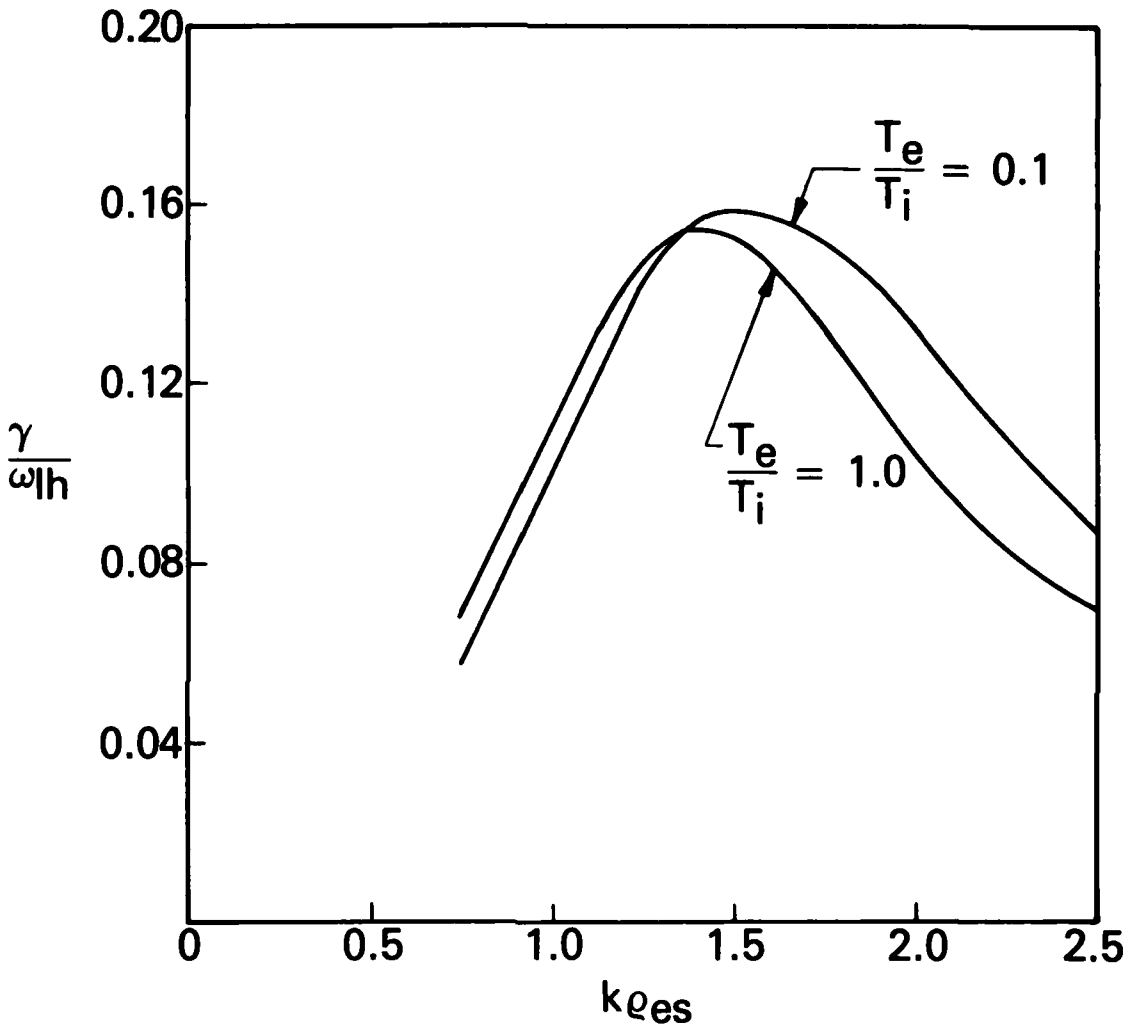

Figure 3

Plot of $\gamma/\omega_{\ell h}$ vs. $k\rho_{es}$ for $V_{di}/v_i = 1.0$, $\omega_{pe}/\Omega_e = 10.0$, $L_n/L_s = 0.1$, $\beta = 0.2$ and $T_e/T_i = 0.1$ and 1.0.

electron VB drift-wave resonance causes weaker growth for $T_e/T_i = 1.0$ than $T_e/T_i = 0.1$. This is due to the fact that $V_{Be} \propto T_e$.

In Figs. (4) and (5) we plot the wave potential Q (curve a) and eigenfunctions $\delta\phi$ (curve b) for $V_{di}/v_i = 1.0$, $\omega_{pe}/\Omega_e = 10.0$, $L_n/L_s = 0.1$, $\beta = 0.2$ and $k\rho_{es} = 1.5$ In Fig. (4) we consider $T_e/T_i = 0.1$ and in Fig. (5) we take $T_e/T_i = 1.0$. The eigenvalues for these cases are $\omega/\omega_{\ell h} = 0.83 + i\ 0.16$ for $T_e/T_i = 0.1$ (Fig. 4) and $\omega/\omega_{\ell h} = 0.58 + i\ 0.15$ for $T_e/T_i = 1.0$ (Fig. 5). Although the growth rates for these two cases are comparable (as in Fig 3), examination of the wave potentials (Q) indicates an important difference between the "small" and "large" T_e/T_i limits. First, in Fig. 4a we note that Q_r possesses an "anti-well" character for $x/\rho_{es} < 4.0$ while Q_i is roughly constant. For $x/\rho_{es} > 4.0$ Q_r begins to increase, but is still negative when $\delta\phi$ asymptotes to 0 at $x/\rho_{es} \simeq 7.5$ (Fig. 4b). The eventual increase in Q_r is due to electron Landau damping which would not occur if $T_e = 0$. On the other hand, Q_i increases sharply for $x/\rho_{es} > 2.0$ which is due to the finite growth rate. Thus Fig. 4 indicates that mode localization is primarily due to the outward convection of energy from the region $x = 0$ in the limit $T_e/T_i \to 0$.[6] Stabilization of the mode can occur when the outward propagation of energy is faster then the growth of the mode. On the other hand, for hotter electrons (Fig. 5a), the "anti-well" character of Q_r is only weakly evident for $x/\rho_{es} < 1.0$; for $x/\rho_{es} > 1.0$, Q_r increases and becomes positive for $x/\rho_{es} > 2.2$. The mode is localized within the region $x/\rho_{es} < 5.5$ (Fig. 5b). In this case electron Landau damping is playing the dominant role in the localization of the mode. As the mode propagates outward from $x = 0$, it is rapidly dissipated locally by electron Landau damping Thus Figs. (4) and (5) indicate that different processes

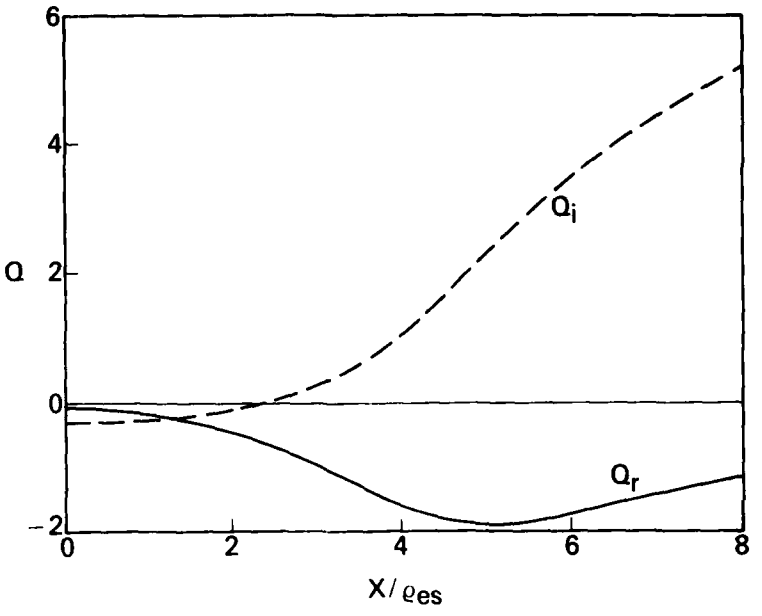

(a)

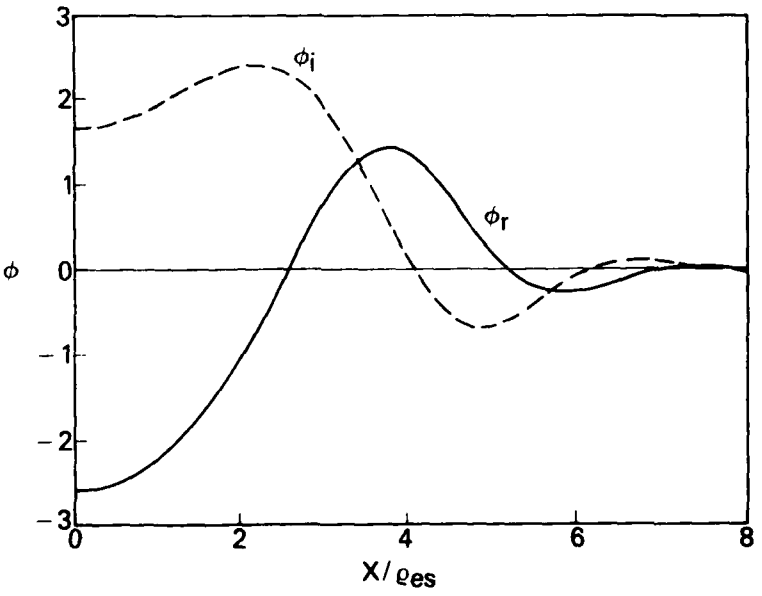

(b)

Figure 4

Plot of the wave potential and eigenfunction for $V_{di}/v_i = 1.0$, $\omega_{pe}/\Omega_e = 10.0$, $L_n/L_s = 0.1$, $\beta = 0.2$, $k\rho_{es} = 1.5$ and $T_e/T_i = 0.1$. The eigenvalue is $\omega/\omega_{\ell h} = 0.83 + i\ 0.16$. The subscripts r and i refer to real and imaginary, respectively. (a) Wave potential Q. (b) Eigenfunction $\delta\phi$.

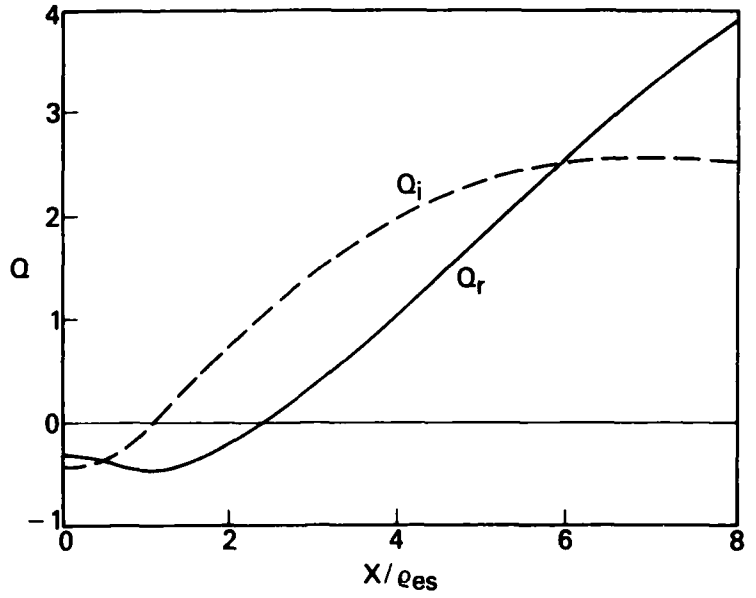

(a)

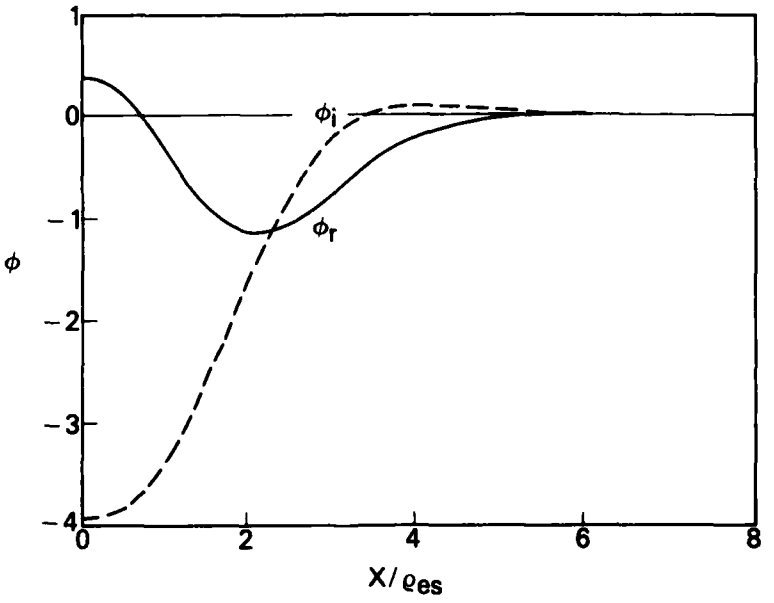

(b)

Figure 5

Plot of the wave potential and eigenfunction for $V_{di}v_i = 1.0$, $\omega_{pe}/\Omega_e = 10.0$, $L_n/L_s = 0.1$, $\beta = 0.2$, $k\rho_{es} = 1.5$ and $T_e/T_i = 1.0$. The eigenvalue is $\omega/\omega_{\ell h} = 0.58 + i\ 0.15$. The subscripts r and i refer to real and imaginary respectively. (a) Wave potential Q. (b) Eigenfunction $\delta\phi$.

are involved in mode localization, depending on the value of T_e/T_i, either outward energy propagation ($T_e << T_i$) or electron Landau damping ($T_e > T_i$) localize the mode.

In Fig. 6 we plot $\gamma/\omega_{\ell h}$ vs. L_n/L_s for $V_{di}/v_i = 1.0$, $\omega_{pe}/\Omega_e = 10.0$, $k\rho_{es} = 1\ 5$, $\beta = 0.0$ and $1\ 0$ and $T_e/T_i = 0.1$ and 1.0. The value of $k\rho_{es}$ chosen correponds roughly to maximum growth. In general, the curves indicate that $\gamma \propto - a(L_n/L_s)+b$, where the slope a and intercept b depend upon β and T_e/T_i. Two important features of this curve are the following. First, for $T_e/T_i = 1.0$, the growth rate for $\beta = 1.0$ is always less then that for $\beta = 0.0$. The value of shear necessary to stabilize the mode for $\beta = 0.0$ is $L_n/L_s = 0.25$ while for $\beta = 1.0$ is $L_n/L_s = 0.17$. Second, for $T_e/T_i = 0.1$, the growth rate for $\beta = 1.0$ is less than that for $\beta = 0.0$ when $L_n/L_s < 0.18$, but is greater than that for $\beta = 0.0$ when $L_n/L_s > 0.18$. Thus as β increases in the low electron temperature limit, the amount of shear necessary to stabilize the mode increases (i.e. L_n/L_s becomes larger); this confirms the result predicted from the analytic theory (Eq. (19)).

In Fig. 7 we plot $\gamma/\omega_{\ell h}$ vs.β for $V_{di}/v_i = 1.0$, $T_e/T_i = 1.0$, $\omega_{\rho e}/\Omega_e = 10.0$, $k\rho_{es} = 1.5$ and various values of L_n/L_s. The main result is that as L_n/L_s increases the growth rate γ decreases, as expected. Also, as L_n/L_s increases, the slopes of the curves change, with a plateau-like structure developing around $\beta \simeq 0.5$.

Finally, we comment on the numerical accuracy of the results presented. Solving Eq. (15) requires a substantial amount of computer time. Typically, 100 - 200 grid points were used in the finite differencing of the differential equation. At each grid point 12 numerical integrations are required to obtain Q. And, in general 5 - 10 interations

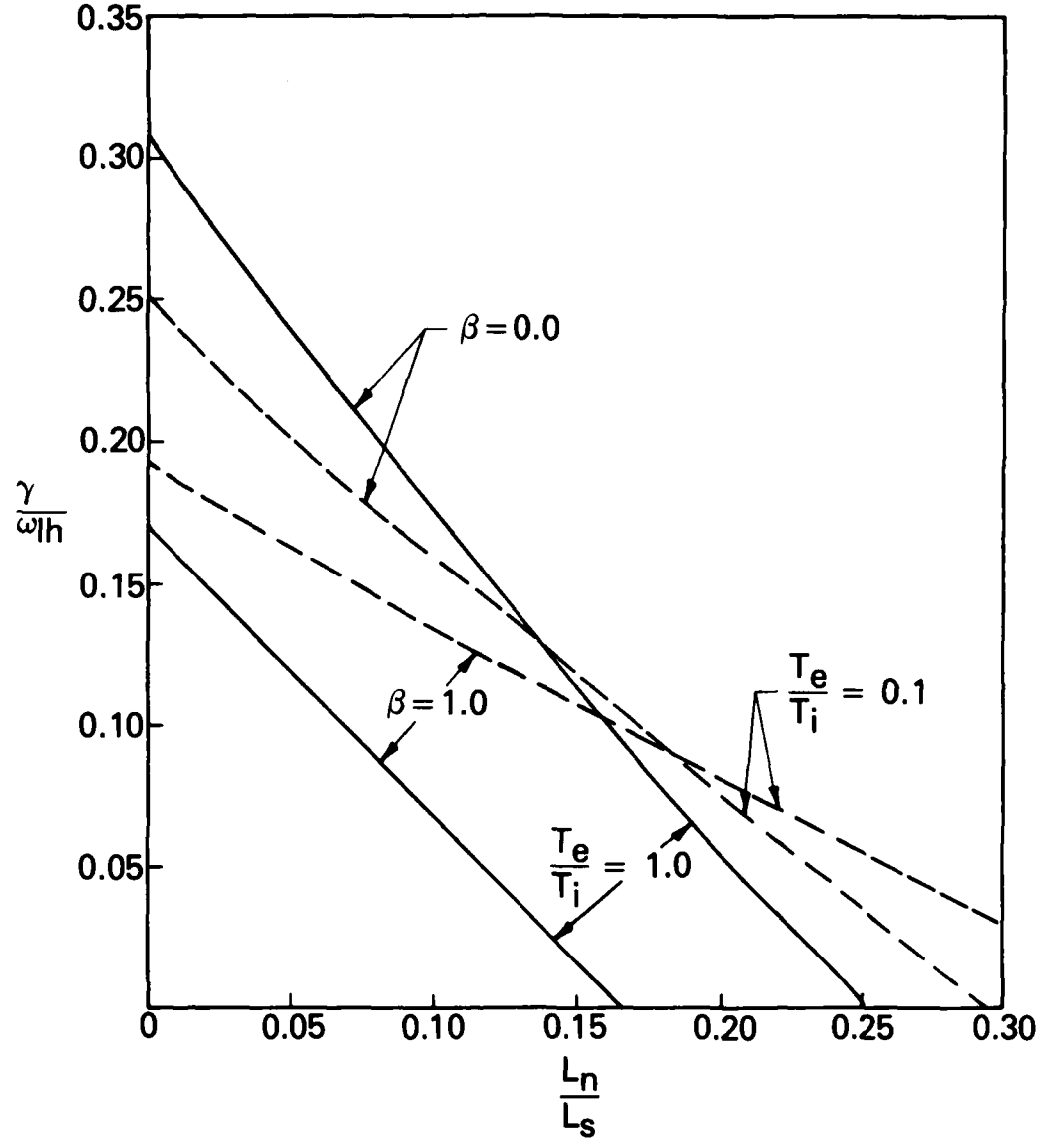

Figure 6

Plot of $\gamma/\omega_{\ell h}$ vs. L_n/L_s for $V_{di}/v_i = 1.0$, $\omega_{pe}/\Omega_e = 10.0$, $k\rho_{es} = 1.5$, $\beta = 0.0$ and 1.0, and $T_e/T_i = 0.1$ and 1.0.

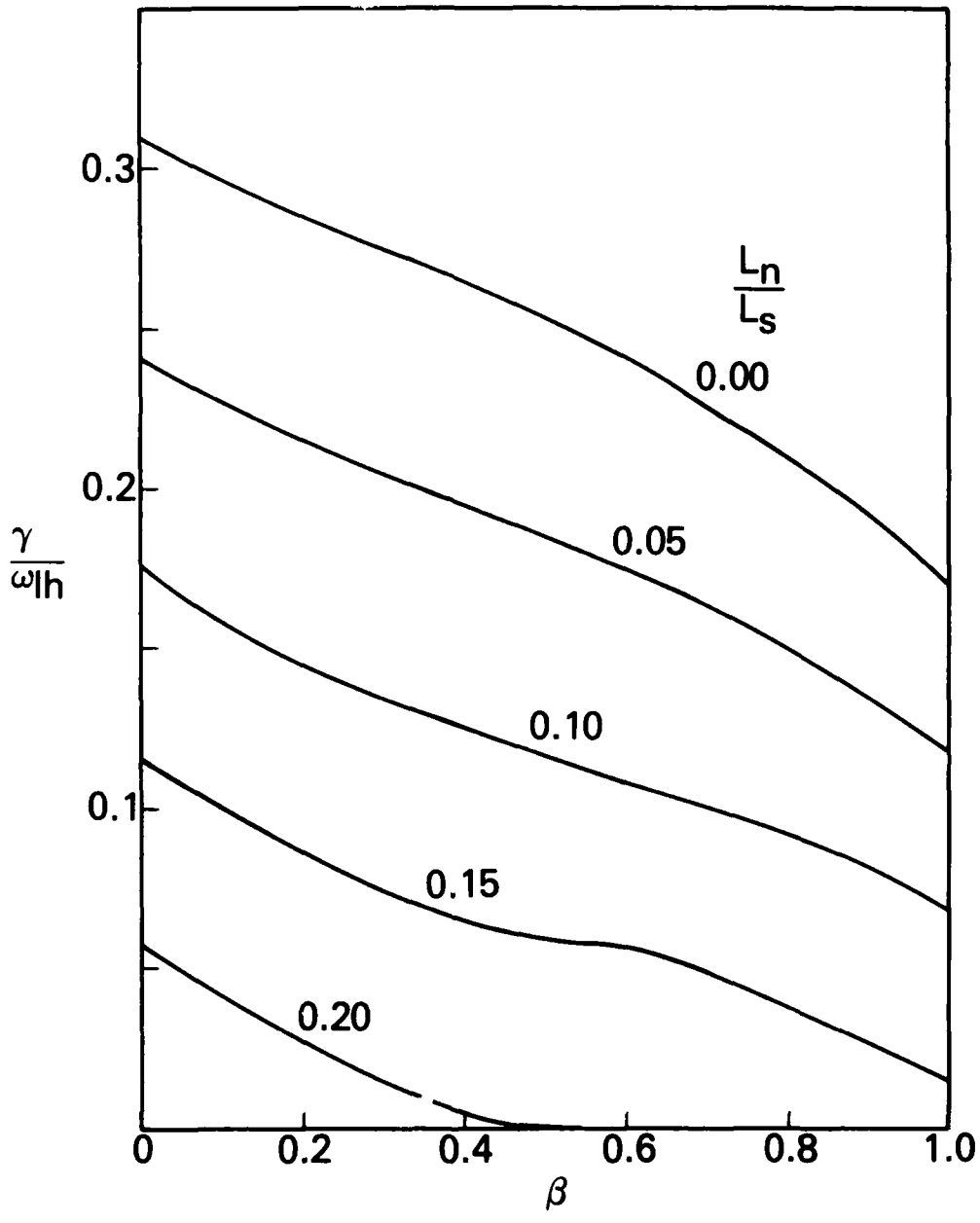

Figure 7

Plot of $\gamma/\omega_{\ell h}$ vs. β for $V_{di}/v_i = 1.0$, $T_e/T_i = 1.0$, $\omega_{pe}/\Omega_e = 10.0$, $k\rho_{es} = 1.5$ and several values of L_n/L_s.

were required to obtain an eigenvalue for a given set of parameters. Thus, approximately 10^4 numerical integrations were needed to obtain a single eigenvalue. In order to minimize the computer time used, some accuracy was sacrificed by using fewer grid points, in both the finite difference scheme and the numerical integrations, than possible. However, higher-resolution grid spacings were used to estimate accuracy for different parameters. We find that the qualitative results presented are reliable, but that the quantitative results are accurate to within 5 - 10% of the actual values.

IV. Discussion

A self-consistent theory of the lower-hybrid-drift instability in a finite β plasma containing magnetic shear has been presented. The theory incorporates the important finite β effects of (1) electrostatic and electromagnetic coupling and (2) electron ∇B drift-wave resonances. The main conclusions of this study are as follows. First, magnetic shear is a strong stabilizing influence on the lower-hybrid-drift instability, which is a well-know result.[14] Second, finite β effects can play an important role in determining the amount of shear necessary for stabilization, as shown by Eq. (19). Interestingly, the two finite β effects mentioned above act in opposing ways. The effect of electromagnetic coupling can be viewed as destabilizing, that is, it tends to increase the amount of shear necessary to stabilize the mode (see $T_e/T_i = 0.1$ curves in Fig. 6). Physically, this occurs because electromagnetic oscillations generate a fluctuating electric field along the magnetic field (due to $\delta A_\parallel$). This inhibits free streaming of electrons along the magnetic field which, therefore, reduces the rate at which energy can be convected away from the localization region. The effect of the electron ∇B drift-wave resonance can be viewed as stabilizing, that is it tends to decrease the amount of shear necessary for stabilization of the mode. This is illustrated in the $T_e/T_i = 1.0$ curves of Fig. 7 and in Fig. 8. Physically, this occurs because the electron ∇B drift-wave resonance is dissipative and reduces growth in the localization region. The key parameter which dictates which finite β effect is dominant is T_e/T_i. Electromagnetic effects dominate when $T_e \ll T_i$, while ∇B resonance effects dominate when $T_e \geq T_i$.

The magnitude of T_e/T_i also plays a role in the nature of the shear stabilization of the lower-hybrid-drift instability. For $T_e \ll T_i$, the

wave potential Q_r has an "anti-well" character.[6] Stabilization occurs because the rate outward energy propagation (away from the localization region) exceeds the growth rate. On the other hand, for $T_e \gg T_i$, the wave potential Q_r has a "well" structure and the wave is dissipated locally by strong Landau damping. This is shown in Figs. (4) and (5).

These results are applicable to reversed field plasmas which contain magnetic shear.[15] Perhaps the simplest example of this is illustrated by the equilibrium

$$\underset{\sim}{B} = B_o \left[\varepsilon \hat{e}_y + \tanh (x/\lambda)\hat{e}_z\right] \tag{22}$$

and

$$n = n_o \operatorname{sech}^2(x/\lambda) \tag{23}$$

where $\varepsilon \ll 1$ Here, the z component of the magnetic component reverses direction at $x = 0$, but the total field remains finite. Studies of the lower-hybrid-drift instability in reversed field plasmas with $\varepsilon = 0$ indicate the following. Based upon a nonlocal linear theory,[19] the fundamental mode is localized away from the neutral line (i e., $x = 0$) at roughly $|x| \gg \lambda$ with a half-width $\Delta x \ll \lambda$. higher order modes also localize about $|x| \simeq \lambda$ but have a much broader half-width, $\Delta x < \lambda$. However, these modes do not penetrate chosen than $|x|_p \sim \lambda(T_e/T_i)^{1/2}$ of the neutral line because of electron ∇B drift-wave resonance damping. Subsequent work on the evolution of a reversed field plasma, using an anomalous resistivity model based upon the nonlocal mode structure of the lower-hybrid-drift instability, found that magnetic flux is transported

towards the neutral line and that the current increase at the neutral line.[20] Thus, the instability can eventually penetrate closer to the neutral line than predicted by linear theory.

If we take $\epsilon \neq 0$, then based on the definitions of L_n and L_s it can be shown that

$$\frac{L_n}{L_s} = -\frac{\epsilon}{\sinh(2x/\lambda)} \cdot \frac{1}{\epsilon^2 + \tanh^2(x/\lambda)} \tag{32}$$

Based on Eq. (31), it is clear that $L_n/L_s \to 0$ in the limit $x/\lambda \to \infty$, while $L_n/L_s \to \infty$ when $x/\lambda \to 0$. Moreover, for this equilibrium

$$\beta = \frac{1}{\cosh^2(x/\lambda)} \cdot \frac{1}{\epsilon^2 + \tanh^2(x/\lambda)} \tag{33}$$

so that $\beta \to 1/\epsilon^2 >> 1$ as $x/\lambda \to 0$. Thus, for $x/\lambda < 1$, both magnetic shear and finite β are important to the stability properties of the lower-hybrid-drift instability in a sheared reversed field plasma. For sufficiently strong magnetic shear (i.e., ϵ) the linear mode penetration distance, $|x|_p$, to the neutral line can be substantially larger than when there is no shear.[15] Thus, magnetic shear can inhibit (or perhaps even prevent) the penetration of the mode to the neutral line even in the nonlinear evolution of the plasma. This can be significant to both laboratory and space plasmas where anomalous diffusion in the field reversal region can be crucial to the dynamics of the plasma.

Acknowledgments

We thank Tom Gladd and Jim Drake for helpful discussions. This research has been supported by ONR and NASA.

References

1. R.C. Davidson and N.T. Gladd, Phys. Fluids, 18 1237 (1975).
2. R.C Davidson, N.T. Gladd C.S. Wu and J.D. Huba, Phys. Fluids 20, 301 (1977).
3. N.A. Krall and P.C. Liewer, Phys. Rev. A4 2094 (1971).
4. R.J. Commisso and H.R. Griem, Phys. Fluids 20, 44 (1977).
5. N.T. Gladd, Y. Goren, C.S. Liu and R.C. Davidson, Phys. Fluids 20, 1876 (1977).
6. R.C. Davidson, N.T. Gladd and Y. Goren, Phys. Fluids 21, 992 (1978).
7. S. Hamasaki and R.K. Linford, Bull. Am. Phys. Soc 24, 1081 (1971).
8. J.D. Huba, N.T. Gladd and K. Papadopoulos, Geophys. Res. Let. 4, 125 (1977).
9. H.U. Fahrbach, W. Koppendorfer M. Munich, J. Neuhauser, H.Rohr, G. Schramm, J. Sommer, and E. Holzhauer, Nuclear Fusion 21, 257 (1981)
10. S P. Gary and T.E. Eastman, J. Geophys. Res. 84, 7378 (1979).
11. J.D. Huba, N.T. Gladd and K. Papadopoulos, J. Geophys. Res 83, 5217 (1978).
12. W.M. Manheimer and J.M. Finn Phys. Fluids 24, 1865 (1981).
13. J.D. Huba, N.T. Gladd and J.F. Drake, J. Geophys. Res. 86, 5881 (1981).
14. N.A. Krall, Phys. Fluids 20, 311 (1977).
15. J.D. Huba, N.T. Gladd and J F. Drake, to be published in J. Geophys. Res. (1982).
16. J.P. Freidberg and R.A. Gerwin, Phys. Fluids 20. 1311 (1977).
17. G. Ganguli and P. Bakshi, Bull. Amer. Phys. Soc. 23, 816 (1978).
18. N.T. Gladd and W. Horton, Jr., Phys. Fluids 16, 879 (1972).
19. J.D. Huba, J.F. Drake and N.T. Gladd, Phys. Fluids 23, 552 (1980).
20. J.F. Drake, N.T. Gladd and J.D. Huba, Phys. Fluids 24, 76 (1981).

Appendix A

We outline the derivation of the perturbed electron density (δn_e) and the perturbed currents (δJ_{xe} and δJ_{ze}) necessary to obtain Eqs. (12) - (14). We first calculate the perturbed distribution function δf_e which is given by

$$\delta f_e = \frac{e}{m_e} \int_{-\infty}^{o} d\tau \exp\,[i \cdot \underset{\sim}{k} \cdot \underset{\sim}{x}'(\tau) - i\omega\tau]\,[-i\underset{\sim}{k}\,\delta\phi + \frac{i\omega}{c}\,\delta\underset{\sim}{A} + \frac{1}{c}\,(\underset{\sim}{v}' \times (i\underset{\sim}{k} \times \delta\underset{\sim}{A}))\,] \cdot \frac{\partial F_{eo}}{\partial \underset{\sim}{v}'} \tag{A1}$$

where $\underset{\sim}{x}'(\tau)$ and $\underset{\sim}{v}'(\tau)$ are the unperturbed orbits. That is,

$$\underset{\sim}{v}'(\tau) = v_\perp \cos(\Omega_e\tau-\theta)\hat{e}_x - [v_\perp \sin(\Omega_e\tau-\theta) + (v_\perp^2/2\Omega_e)\partial\ \ell n\ B/\partial x]\hat{e}_y + v_\parallel \hat{e}_z \tag{A2}$$

$$\underset{\sim}{x}'(\tau) = (v_\perp/\Omega_e)\sin(\Omega_e\tau-\theta)\hat{e}_z + [(v_\perp/\Omega_e)\cos(\Omega_e\tau-\theta) - \tau(v_\perp^2/2\Omega_e)\partial\ \ell n\ B/\partial x]\hat{e}_y + v_\parallel \tau\,\hat{e}_z \tag{A3}$$

where $v_\perp^2 = v_x^2 + v_y^2$ and $\Omega_e = e\,B/m_e c$. The unperturbed electron distribution function is chosen to be

$$F_{eo} = n\,(\pi v_e^2)^{-3/2}\,[1 - \frac{v_y}{\Omega_e}\frac{\partial\ \ell n\ n}{\partial x}]\exp\,[-v^2/v_e^2] \tag{A4}$$

where $v_e^2 = 2T_e/m_e$ and $v^2 = v_x^2 + v_y^2 + v_z^2$.

Substituting Eqs. (A2) - (A4) into (A1) and performing the temporal

integration we arrive at

$$\delta f_e = \frac{2e}{m_e v_e^2} \left[\left(\delta\phi + \frac{\omega}{ck_y} \left(\frac{k}{k_y} \delta A_x + \frac{k_z}{k_y} \delta A_z \right) \right) \right.$$

$$- \sum_{n,m} \exp\left[i(\phi - \psi - \frac{\pi}{2})(n-m) \right] R_e \left\{ J_n J_m \delta\phi \right. \tag{A5}$$

$$+ \left\{ \frac{\omega - k_z v_z}{ck_y} \frac{k_x}{k_y} J_n J_m + \frac{v_\perp}{c} \frac{k_\perp^2}{k_y^2} \left(i \cos\psi J_n' J_m - \frac{n}{\sigma} J_n J_m \sin\psi \right) \right\} \delta A_x$$

$$\left. + \left\{ \left(\frac{\omega}{ck_y} \frac{k_z}{k_y} - \frac{v_z}{c} \left(1 + \frac{k_z^2}{k_y^2} \right) \right) J_n J_m + \frac{v_\perp}{c} \frac{k_x}{k_y} \frac{k_z}{k_y} \left(i \cos\psi J_m J_n' - \frac{n}{\sigma} J_n J_m \sin\psi \right) \right\} \delta A_z \right]$$

where $R_e = (\omega - k_y V_{de})/(\omega - n\Omega_e - k_y V_{Be}(v_\perp^2/v_e^2) - k_x v_z)$, $\psi = \tan^{-1}(k_x/k_y)$, the argument of the Bessel functions is $\sigma = k_\perp v_\perp/\Omega_e$, $V_{de} = -(v_e^2/2\Omega_e)\partial \ell n\, n/\partial x$, $V_{Be} = -(v_e^2/2\Omega_e)\partial \ell n\, B/\partial x$, and $v_e^2 = 2T_e/m_e$.

The perturbed electron density and current are defined as

$$\delta n_e = \int d^3v\, \delta f_e \tag{A6}$$

$$\delta \underset{\sim}{J}_e = \int d^3v\, \underset{\sim}{v}\, \delta f_e \,. \tag{A7}$$

Making use of Eq. (A5) in Eqs. (A6) and (A7) we obtain

$$\delta n_e = -(2\pi e\ \lambda_{de}^2)^{-1}\left[\left(\delta\phi + \frac{\omega}{ck_y}\left(\frac{k_x}{k_y}\delta A_x + \frac{k_z}{k_y}\delta A_z\right)\right)\right.$$

$$+\Lambda \int_o^\infty d(u^2)\ \exp(-u^2)\ \{J_o^2\ Z\ \delta\phi \qquad \text{(A8)}$$

$$+ \left(\frac{k_x}{k_y} J_o^2 \left(\frac{\omega}{ck_y} Z + \frac{k_z}{k_y}\frac{v_e}{c}\frac{1}{2} Z'\right) - i\ \frac{v_e}{c}\frac{k_\perp^2}{k_y^2}\cos\psi\ J_o J_1\ \zeta_e Z\right)\delta A_x$$

$$\left. + \left(\frac{\omega}{ck_y} J_o^2 \left(\frac{k_z}{k_y} Z + \frac{k_y v_e}{\omega}\left(1+\frac{k_z^2}{k_y^2}\right)\frac{1}{2} Z' - i\ \frac{v_e}{c}\frac{k_z}{k_y}\frac{k_x}{k_y} J_o J_1 \cos\psi\zeta Z\right)\delta A_z\right]$$

$$\delta J_{xe} = -\left(2\pi e\ \lambda_{de}^2\right)^{-1} v_e \Lambda \int_o^\infty d(u^2)\ u\ \exp(-u^2)\ \left[-i\ J_o J_1 \cos\psi\ Z\ \delta\phi \qquad \text{(A9)}\right.$$

$$+ \left\{-i\ \frac{}{}\left(\frac{k_x}{k_y} Z + \frac{\omega}{ck_y}\frac{k_z}{k_y}\frac{v_e}{c} Z\frac{1}{2}\right) J_o' J_1 \cos\psi - \frac{v_e}{c}\frac{k_\perp^2}{k_y^2} J_1^2 \cos^2\psi\zeta Z\right\}\delta A_x$$

$$\left. + \left\{-i\ \frac{\omega}{ck_y}\left(\frac{k_z}{k_y} Z + \frac{k_y v_e}{\omega}\left(1 + \frac{k_z^2}{k_y^2}\right)\frac{1}{2} Z'\right) J_o J_1 \cos\psi - \frac{v_e}{c}\frac{k_x}{k_y}\frac{k_z}{k_y} J_1^2 \cos\psi\delta Z\right\}\zeta A_z\right]$$

$$\delta J_{ze} = (2\pi e\ \lambda_{de}^2)^{-1} v_e\ \Lambda \int_o^\infty d(u^2)\ \exp(-u^2)\ \left[J_o^2\ Z'\delta\phi\right.$$

$$+\left\{\frac{\omega}{ck_y}\frac{k_x}{k_y} J_o^2 Z'\left(1 - \frac{k_y v_e}{\omega}\zeta\right) - i\ J_o J_1 \frac{v_e}{c}\frac{k_\perp^2}{k_y^2}\cos\psi\ Z'\right\}\delta A_x \qquad \text{(A10)}$$

$$\left. + \left\{\frac{\omega}{ck_y}\left(\frac{k_z}{k_y} - \frac{k_y v_e}{\omega}\left(1 + \frac{k_z^2}{k_y^2}\right)\zeta\right) J_o^2 Z - i\cos\psi\ J_o J_1\ \frac{v_e}{c}\frac{k_x}{k_y}\frac{k_z}{k_y}\zeta Z'\right\}\delta A_z\right]$$

where $\Lambda = (\omega - k_y V_{de})/k_z v_e$, $u = v_\perp/v_e$, the argument of the Bessel functions is $\sigma = (k_\perp v_e/\Omega_e)u$, the argument of the Z functions is $\zeta_e = (\omega - k_y V_{Be} u^2)/k_z v_e$ and $\lambda_{de}^2 = v_e^2/2\omega_{pe}^2$. In writing Eqs. (A8) - (A10) we have retained only the $n = 0$ term in the summation over cyclotron harmonics since $\omega << \Omega_e$.

The perturbed ion density in an unmagnetized plasma is simply

$$\delta n_i = -\frac{n_o}{T_i}\left[1 + \zeta_i\, Z(\zeta_i)\right]$$

where $\zeta_i = (\omega - kV_{di})/kv_i$, $V_{di} = (v_i^2/2\Omega_i)\partial\ \ell n\ n/\partial x$ and $v_i^2 = 2T_i/m_i$.

Appendix B

We outline the derivation of Eq. (15) and present the detailed form of p and q used in the analysis. Substituting δn_α and $\delta \underset{\sim}{J}_e$, derived in the Appendix A, into the Maxwell equations (Eqs. (10) and (11)) we obtain the following set of equations

$$D_{\phi\phi}\ \delta\phi + \frac{k}{k_y} D_{\phi x}\ \delta A_x + D_{\phi z}\ \delta A_z = 0 \tag{B1}$$

$$\frac{k_y}{k} D_{x\phi}\ \delta\phi + D_{xx}\ \delta A_x + \frac{k_y}{k} D_{xz}\ \delta A_z = 0 \tag{B2}$$

$$D_{z\phi}\ \delta\phi + \frac{k}{k_y} D_{zx}\ \delta A_x + D_{zz}\ \delta A_z = 0 \tag{B3}$$

where

$$D_{\phi\phi} = 1 + \frac{1}{k_y^2\ \lambda_{de}^2} \frac{T_e}{T_i} (1 + \zeta_i\ Z(\zeta_i)) + \frac{1}{k_y^2\ \lambda_{de}^2} (1 + K_{\phi\phi}) \tag{B4}$$

$$D_{\phi x} = D_{x\phi} = i\ \frac{1}{k_y \lambda_{de}} \frac{\sqrt{2}\omega_{pe}}{ck_y} K_{\phi x} \tag{B5}$$

$$D_{\phi z} = -\ D_{z\phi} = \frac{1}{k_y \lambda_{de}} \frac{\sqrt{2}\omega_{pe}}{ck_y} K_{\phi z} \tag{B6}$$

$$D_{xx} = 1 - \frac{2\omega_{pe}^2}{c^2 k_y^2} K_{xx} \tag{B7}$$

$$D_{xz} = -\ D_{zx} = i\ \frac{2\omega_{pe}^2}{c^2 k_y^2} K_{xz} \tag{B8}$$

$$D_{zz} = 1 + \frac{2\omega_{pe}^2}{c^2 k_y^2} K_{zz} \tag{B9}$$

and

$$K_{\phi\phi} = \Lambda \int_o^\infty d(u^2)\, \exp(-u^2)\, J_o^2\, (k_\perp r_{Le} u)\, Z\, (\zeta_e) \tag{B10}$$

$$K_{\phi x} = \Lambda \int_o^\infty d(u^2)\, \exp(-u^2)\, u\, J_o\, (k_\perp r_{Le} u)\, J_1\, (k_\perp r_{Le} u)\, Z\, (\zeta_e) \tag{B11}$$

$$K_{\phi z} = \Lambda \int_o^\infty d(u^2)\, \exp(-u^2)\, J_o^2\, (k_\perp r_{Le} u)\, \frac{1}{2}\, Z'\, (\zeta_e) \tag{B12}$$

$$K_{xx} = \Lambda \int_o^\infty d(u^2)\, \exp(-u^2)\, u^2\, J_1^2\, (k_\perp r_{Le} u)\, Z\, (\zeta_e) \tag{B13}$$

$$K_{xz} = \Lambda \int_o^\infty d(u^2)\, \exp(-u^2)\, u\, J_o(k_\perp r_{Le} u)\, J_1(k_\perp r_{Le} u)\, \frac{1}{2}\, Z'\, (\zeta_e) \tag{B14}$$

$$K_{zz} = \Lambda \int_o^\infty d(u^2)\, \exp(-u^2)\, J_o^2(k_\perp r_{Le} u)\, \frac{1}{2}\, \zeta_e\, Z'\, (\zeta_e)\,. \tag{B15}$$

In the above,

$$\Lambda = \frac{\omega - k_y V_{de}}{k_z v_e}$$

$$\zeta_e = \frac{\omega - k_y V_{Be} u^2}{k_z v_e}; \quad \zeta_i = \frac{\omega - k_y V_{di}}{k v_i}; \quad V_{di} = \frac{v_i^2}{2\Omega_i} \frac{\partial\, \ell n\, n}{\partial x}$$

$$V_{de} = -\frac{v_e^2}{2\Omega_e} \frac{\partial\, \ell n\, n}{\partial x}; \quad V_{Be} = -\frac{v_e^2}{2\Omega_e} \frac{\partial\, \ell n\, B}{\partial x} = -\frac{\beta}{2}\, V_{de}$$

$u = v_\perp / v_e$, $\lambda_{de}^2 = v_e^2 / \partial \omega_{pe}^2$, $v_e^2 = 2T_e/m_e$, $\omega_{pe}^2 = 4\pi\, ne^2/m_e$, $r_{Le} = v_e/\Omega_e$, J_n is the Bessel function of order n, $Z' = dZ/d\zeta$, $k_\perp^2 = k_x^2 + k_y^2$, and $k_z = k_y (x/L_s)$.

We expand $\underline{\underline{D}}$ in the small parameter k_x^2/k_y^2 and find that

$$\underline{\underline{D}} = \underline{\underline{D}}^{(0)} + \underline{\underline{D}}^{(2)} \left(\frac{k_x^2}{k_y^2}\right) \tag{B16}$$

where $\underset{\approx}{D}^{(0)}$ are given by Eqs. (B4) - (B15) with $k_\perp$ replaced by k_y and

$$D_{\phi\phi}^{(2)} = 1 - \frac{1}{k_y^2 \lambda_{de}^2} \frac{T_e}{T_i} \frac{1}{2} \zeta_i (\zeta_i Z(\zeta_i))' + \frac{1}{k_y^2 \lambda_{de}^2} K_{\phi\phi}^{(2)} \tag{B17}$$

$$D_{\phi z}^{(2)} = D_{z\phi}^{(2)} = i \frac{1}{k_y \lambda_{de}} \frac{\sqrt{2}\omega_{pe}}{ck_y} K_{\phi x}^{(2)} \tag{B18}$$

$$D_{\phi z}^{(2)} = - D_{z\phi}^{(2)} = \frac{1}{k_y \lambda_{de}} \frac{\sqrt{2}\omega_{pe}}{ck_y} K_{\phi x}^{(2)} \tag{B19}$$

$$D_{xx}^{(2)} = 1 - \frac{2\omega_{pe}^2}{c^2 k_y^2} K_{xx}^{(2)} \tag{B20}$$

$$D_{xz}^{(2)} = - D_{zx}^{(2)} = i \frac{2\omega_{pe}^2}{c^2 k_y^2} K_{xz}^{(2)} \tag{B21}$$

$$D_{zz}^{(2)} = 1 + \frac{2\omega_{pe}^2}{c^2 k_y^2} K_{zz}^{(2)} \tag{B22}$$

and

$$K_{\phi\phi}^{(2)} = - \Lambda k_y r_{Le} \int_o^\infty d(u^2) \exp(-u^2)\, u\, J_o J_1 Z(\zeta_e) \tag{B23}$$

$$K_{\phi x}^{(2)} = \Lambda \frac{1}{2} k_y r_{Le} \int_o^\infty d(u^2) \exp(-u^2) u^2 [J_o J_1' - J_1^2)]\, Z(\zeta_e) \tag{B24}$$

$$K_{\phi z}^{(2)} = - \Lambda k_y r_{Le} \int_o^\infty d(u^2) \exp(-u^2) u J_o J_1 \frac{1}{2} Z'(\delta_e) \tag{B25}$$

$$K_{xx}^{(2)} = \Lambda k_y r_{Le} \int_o^\infty d(u^2) \exp(-u^2) u^3 J_1 J_1' Z(\zeta_e) \tag{B26}$$

$$K_{xz}^{(2)} = \Lambda \frac{1}{2} k_y r_{Le} \int_o d(u^2) \exp(-u^2) u^2 [J_o J_1' - J_1^2] \frac{1}{2} Z'(\zeta_e) \tag{B27}$$

$$K_{zz}^{(2)} = -\Lambda k_y r_{Le} \int_0^\infty d(u^2)\exp(-u^2)uJ_0J_1 \frac{1}{2}\zeta_e Z(\zeta_e') \tag{B28}$$

and the argument of the Bessel functions is $k_y r_{Le} u$.

We now solve Eqs. (B2) and (B3) for δA_x and δA_z in terms of $\delta\phi$. We find that

$$\delta A_x = -\frac{k_y}{k}\frac{D_{\phi x} D_{zz} + D_{xz} D_{\phi z}}{D_{xx} D_{zz} + D_{xz}^2}\delta\phi \tag{B29}$$

$$\delta A_z = \frac{D_{\phi z} D_{xx} - D_{xz} D_{\phi z}}{D_{xx} D_{zz} + D_{xx}^2}\delta\phi \tag{B30}$$

Substituting (B1o) into (B29) and (B30), and then substituting (B29) and (B30) into (B1) we obtain, to lowest order in k_x^2/k_y^2,

$$p(\omega,k_y,x)\frac{\partial^2\delta\phi}{\partial x^2} - q(\omega,k_y,x)\,k_y^2\,\delta\phi = 0 \tag{B31}$$

where

$$p = D_{\phi\phi}^{(2)} - D_{\phi x}\left(\Gamma_{nx}^{(0)}/\Gamma_{dx}^{(0)}\right) + D_{\phi z}^{(2)}\left(\Gamma_{nx}^{(0)}/\Gamma_{dx}^{(0)}\right) \tag{B32}$$

$$- D_{\phi x}^{(0)}\left(\Gamma_{nx}^{(2)}\,\Gamma_{dx}^{(0)} - \Gamma_{nx}^{(0)}\,\Gamma_{dx}^{(2)}\right)/\Gamma_{dx}^{(0)\,2}$$

$$+ D_{\phi z}^{(0)}\left(\Gamma_{nz}^{(2)}\,\Gamma_{dz}^{(0)} - \Gamma_{nz}^{(0)}\Gamma_{dz}^{(0)}\right)/\Gamma_{dz}^{(0)2}$$

$$q = D_{\phi\phi}^{(0)} - D_{\phi x}^{(0)}\left(\Gamma_{nx}^{(0)}/\Gamma_{dx}^{(0)}\right) + D_{\phi z}^{(0)}\left(\Gamma_{nz}^{(0)}/\Gamma_{dz}^{(0)}\right) \tag{B33}$$

and

$$\Gamma_{nx}^{(0)} = D_{\phi x}^{(0)} D_{zz}^{(0)} + D_{xz}^{(0)} D_{\phi x}^{(0)} \tag{B34}$$

$$\Gamma_{nx}^{(2)} = D_{\phi x}^{(2)} D_{zz}^{(0)} + D_{xz}^{(2)} D_{\phi z}^{(0)} + D_{xz}^{(0)} D_{\phi z}^{(2)} - D_{xx}^{(2)} D_{xz}^{(0)} D_{\phi z}^{(0)}/D_{zz}^{(0)} \tag{B35}$$

$$\Gamma_{dx}^{(0)} = \Gamma_{dz}^{(0)} = D_{xx}^{(0)} D_{zz}^{(0)} + D_{xz}^{(0)2} \tag{B36}$$

$$\Gamma_{dx}^{(2)} = D_{xx}^{(2)} D_{zz}^{(0)} + 2 D_{xz}^{(0)} D_{xz}^{(2)} - D_{xz}^{(0)2} D_{zz}^{(2)}/D_{zz}^{(0)} \tag{B37}$$

$$\Gamma_{nz}^{(0)} = D_{\phi z}^{(0)} D_{xx}^{(0)} - D_{xz}^{(0)} D_{ox}^{(0)} \tag{B38}$$

$$\Gamma_{nz}^{(2)} = D_{oz}^{(2)} D_{xx}^{(0)} - D_{xz}^{(2)} D_{\phi x}^{(0)} - D_{xz}^{(0)} D_{\phi x}^{(2)} + D_{xz}^{(0)} D_{\phi x}^{(0)}/D_{xx}^{(0)} \tag{B39}$$

$$\Gamma_{dz}^{(2)} = D_{zz}^{(2)} D_{xx}^{(0)} + 2D_{xz}^{(0)} D_{xz}^{(2)} - D_{xz}^{(0)2} D_{xx}^{(2)}/D_{xx}^{(0)} \tag{B40}$$

and we have mode the identification $k_x^2 = -\partial^2/\partial x^2$.